ANALYSIS OF SOLIDIFICATION CRACKING CONSIDERING MECHANICAL AND METALLURGICAL FACTORS

S. MAEDA*, T. KATO*, K. IKUSHIMA*, M. SHIBAHARA*

**Graduate School of Engineering, Osaka Metropolitan University, Osaka, Japan*

DOI 10.3217/978-3-85125-968-1-24

ABSTRACT

The introduction of tack welding by large-heat-input welding instead of using an out-of-plane constraint has been considered for butt welding automation. However, the occurrence of solidification cracking in welding is a major issue in large-heat-input welding. Solidification cracking is a welding defect that can significantly reduce the strength of weld joints and structures; therefore, it is important to predict its occurrence for its prevention. Solidification cracking is a phenomenon caused by the interaction of mechanical and metallurgical factors and it is known to have a tendency to occur where columnar crystals collide. In the present study, we proposed a numerical analysis method to evaluate the occurrence of solidification cracking in welding using the thermal elastic-plastic analysis using finite element method (FEM) while considering mechanical and metallurgical factors. As a mechanical factor, a cracking evaluation index using the increment of plastic strain that occurs in the solidification brittle temperature range (BTR) during the cooling process is proposed. As a metallurgical factor, the solidification shrinkage strain and the strength of the solid-liquid coexistence region that changes with the solid fraction are modelled. In addition, we proposed a simplified method for predicting the direction of columnar crystal growth using temperature gradients in the BTR. The proposed method was applied to butt welding, and the effect of welding conditions on solidification crack generation was investigated. It was found that the direction of columnar crystal growth predicted by the simplified method using temperature gradient in the BTR was in good agreement with the experimental results. In addition, the crack generation positions obtained with an evaluation index using the plastic strain increment in the BTR were in good agreement with the cracking positions observed in experiments. The influence of the solidification shrinkage strain on solidification crack generation was examined in terms of the relation between the collision angle of columnar crystals and the restraining state around the melting part. Based on these results, it can be concluded that the effects of mechanical and metallurgical factors on solidification cracking in welding can be analysed using the proposed method.

Keywords: Solidification cracking in welding, Thermal elastic-plastic FEM, Plastic strain increment in the BTR, Solid fraction, Solidification shrinkage, Crystal growth direction.

INTRODUCTION

In recent years, the Japanese shipbuilding industry has been attempting to automate welding due to the difficulty in securing welding workers [1]. This is partly due to the increase in welding operations as vessels have become larger in order to reduce transportation costs. In automated welding, as shown in Fig. 1, the out-of-plane constraint

is required to be changed to in-plane tack welding from the viewpoint of operability. In this case, it is necessary to re-melt the in-plane tack welding from the viewpoint of weld quality, and welding with a large heat input is required. However, there is concern about the occurrence of weld solidification cracking during large-heat-input welding [2]. Weld solidification cracking is a welding defect that occurs when large tensile strain is applied in the temperature range just below the melting point of the weld metal as it solidifies and can significantly reduce the integrity of the weld part [3-5]. Therefore, non-destructive testing is performed after welding on welds where cracking is likely to occur, and if cracking is confirmed, then repair welding is performed, which is one of the reasons for the increase in manufacturing costs. Thus, it is important to establish an analytical method that can predict the occurrence of weld solidification cracking and study the effects of various factors.

In the present study, a solidification cracking analysis method that can take into account metallurgical solidification phenomena and mechanical strain behaviour in the molten part is proposed. As a metallurgical factor, the relationship between the brittle temperature range (BTR) and the solid fraction determined from the metal composition and the solidification shrinkage strain calculated from the solid fraction are considered in the evaluation of BTR plastic strain by the thermal elastic-plastic analysis using finite element method (FEM). A simple method for predicting the direction of columnar crystal growth, which affects the location of solidification cracking, is also proposed using the temperature gradient. And proposed method is used to evaluate the collision angle at which columnar crystals collide with each other.

Then, the developed method is applied to large-heat-input butt welding in order to demonstrate the validity of the proposed method through comparison with experimental results. In addition, the effects of welding deformation as a mechanical factor and solidification shrinkage strain as a metallurgical factor on the solidification cracking are also discussed.

Through the above studies, we show the utility of the plastic strain increment in the BTR for the evaluation of solidification cracking initiation and clarify that the crack initiation location can be predicted by considering both mechanical and metallurgical factors.

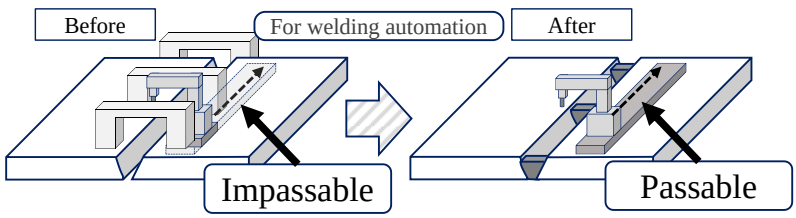

Fig. 1 Transition of constraint states for butt welding automation

HOT CRACKING ANALYSIS METHOD

The occurrence of weld solidification cracking is affected by phenomena associated with both the solidification of the molten metal and the welding deformation of the entire member due to locally large heat input.

In the present study, we propose a solidification cracking analysis method that can take into account the effects of metallurgical and mechanical factors using thermal elastic-plastic analysis using FEM, which is used to analyse weld deformation and residual stresses. Specifically, the shrinkage associated with the solidification in the BTR and the strength of the molten metal are considered in thermal elastic-plastic analysis using FEM while reproducing the progress of solidification based on the relationship between the solid fraction and temperature in the BTR. An evaluation index for solidification cracking using the plastic strain in the BTR is also proposed. In addition, we propose a simple method for predicting the direction of columnar crystal growth, which has a significant influence on the occurrence of solidification cracking in heat conduction FEM. Since the solidification cracking analysis requires the detailed elements in the weld part, an efficient simulation was achieved using a large-scale thermal elastic-plastic analysis method referred to as the idealized explicit finite element method (IEFEM) [6].

This section describes the details of the analysis method for solidification cracking proposed by authors.

MATERIAL CONSTANTS FOR HOT CRACKING ANALYSIS

In thermal elastic-plastic analysis using FEM, the temperature and mechanical fields from the heating process to the cooling process by welding are sequentially analysed based on the temperature dependency of the material properties. Fig. 2 shows the temperature dependent material properties of Japanese Industrial Standards G 3106 SM490A [7]. In the present study, in addition to setting the material properties used in general welding mechanics analysis, a method for setting material properties in the BTR was proposed for the analysis of solidification cracking.

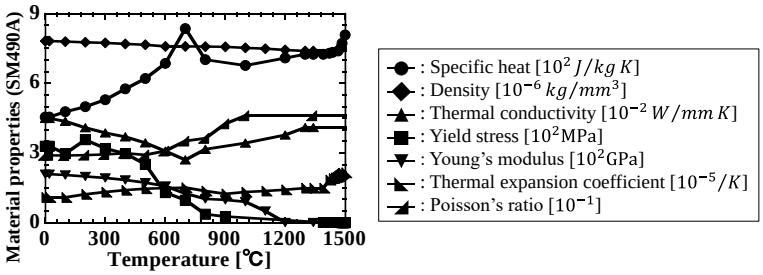

Fig. 2 Temperature dependent material properties of Japanese Industrial Standards G 3106 SM490A [7]

Relationship between temperature and solid fraction

In solidification cracking analysis, it is necessary to consider the progress of solidification of the molten metal. In the present study, the progress of solidification was represented by determining the solid fraction of each element from the temperature obtained by the heat conduction FEM. Table 1 shows the chemical composition of JIS G 3106 SM490A [7].

In the present study, the three elements shown in Table 2 were used in a simplified calculation model of micro-segregation proposed by Clyne et al [8]. The derived relationship between the temperature and the solid fraction is shown in Fig. 3. The figure shows that the BTR is 110°C, from 1390°C to 1500°C.

Table 1 Chemical composition of JIS G 3106 SM490A [7]

Composition	C	Si	Mn	P	S
(wt%)	0.16	0.24	1.51	0.012	0.005

Table 2 Thermophysical data [8]

Element		k	D	α	m_i	C_0
C	δ	0.200	6.4e-3	64	90	0.160
	γ	0.360	6.4e-4	6.4	70	
P	δ	0.130	4.0e-5	0.4	50	0.012
	γ	0.060	2.5e-6	0.025	50	
S	δ	0.060	1.6e-4	1.6	20	0.005
	γ	0.015	3.9e-5	0.39	20	

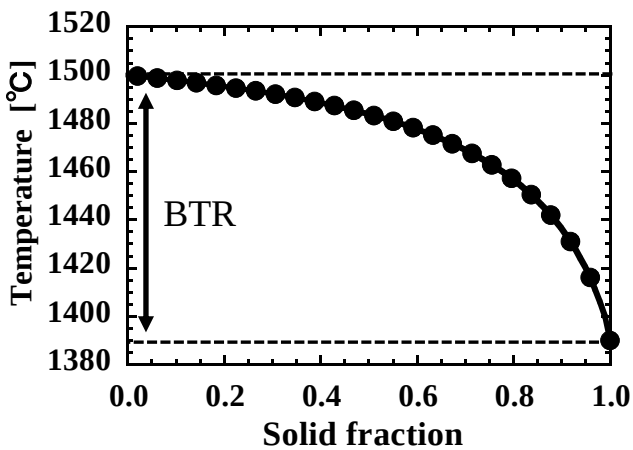

Fig. 3 Relationship between temperature and solid fraction in BTR

Solidification shrinkage strain

During solidification of a molten metal, the liquid phase is pulled toward the solid phase due to the solidification shrinkage strain ε_{sh} caused by the density difference between the liquid and solid metals. Specifically, in carbon steel, it is known that there is a density difference of approximately 3.0% [9,10] and its influence cannot be ignored compared to the critical strain for crack initiation [11]. This causes a solidification shrinkage strain of approximately 1.0 % in one direction.

The increment of the solidification shrinkage strain $\Delta\varepsilon_{sh}$ when the solid fraction f_s changes in the BTR can be expressed as follows:

$$\Delta\varepsilon_{sh} = \Delta f_s \left(\frac{\rho_s}{\rho_l} - 1 \right) \tag{1}$$

where ρ_s is the density of solid, ρ_l is the density of liquid, and (ρ_s /ρ_l -1) on the right-hand side is the solidification shrinkage coefficient [12,13].

In the present study, (ρ_s/ρ_l -1) is defined as 0.03, and, based on the relationship between temperature and solid fraction shown in Fig. 3, solidification shrinkage is considered as thermal strain by introducing the increment of solidification shrinkage strain into the thermal expansion coefficient, as shown in Fig. 2.

Strength of molten metal

When considering shrinkage around molten metal, it is important to reproduce the difference in strength between solid and liquid metals. For example, rather than the solid phase which has higher strength, the liquid phase which has lower strength, is tensile due to solidification shrinkage.

It has been confirmed through high-temperature tensile tests that molten metals can retain a stress of approximately 1.0 MPa near the solidus temperature due to partial crystal bonding caused by solidification [14]. Therefore, the yield stress at 1390°C, which is the solidus temperature, was set to 1.0 MPa in the present study. In the temperature range above the liquidus temperature, the strength of the molten metal is considered to be approximately zero. It is thought that the strength of the molten metal can be reproduced by making the yield stress very small above the liquidus temperature in the thermal elastic-plastic analysis using FEM. However, if the yield stress is set to be too small, the analysis becomes unstable. In the present study, therefore, a value of 0.1 MPa, which is sufficiently smaller than 1.0 MPa, was used. In the BTR, the yield stress is assumed to be proportional to the solid phase ratio, as shown in Fig. 4.

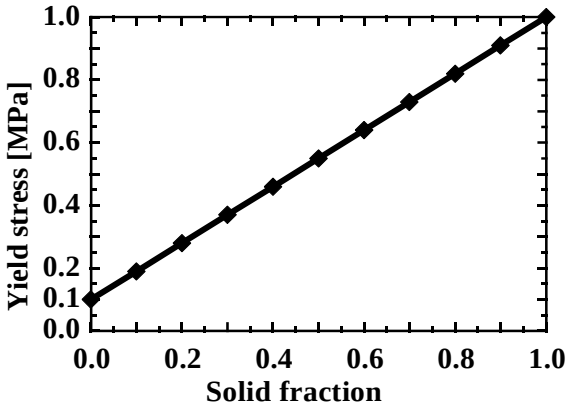

Fig. 4 Relationship between Yield stress in BTR and solid fraction

HOT CRACKING EVALUATION INDEX

Solidification cracking is evaluated by the displacement and strain acting on the weld metal in the BTR, and cracking occurs when these values exceed the critical ductility curve, as shown in Fig. 5 [15]. In other words, the amount of strain generated in the BTR is important to evaluate the occurrence of solidification cracking.

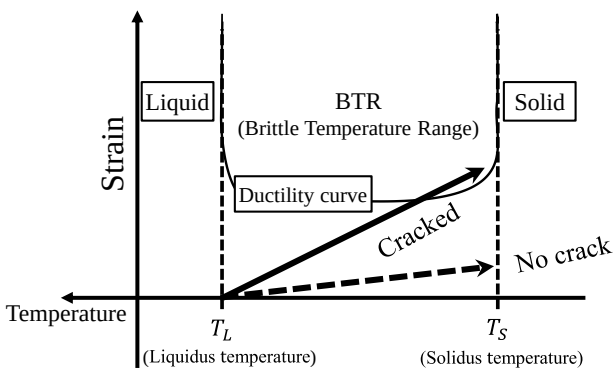

Fig. 5 Schematic illustration of initiation of solidification cracking

Strain in the thermal elastic-plastic analysis using FEM is defined as the strain used in ordinary elastic-plastic analysis and the thermal strain. In addition to these strains, it is necessary to consider the solidification shrinkage strain associated with the solidification of the molten metal in solidification cracking analysis, as described above. In other words, the total strain increment is the sum of the elastic strain increment $\Delta\varepsilon^{e}$, the plastic strain increment $\Delta\varepsilon^{p}$, the thermal strain increment $\Delta\varepsilon^{T}$ and the solidification shrinkage strain increment $\Delta\varepsilon^{sh}$, as shown in the following equation:

$$\Delta\varepsilon = \Delta\varepsilon^{e} + \Delta\varepsilon^{p} + \Delta\varepsilon^{T} + \Delta\varepsilon^{sh} \tag{2}$$

On the other hand, solidification shrinkage is a phenomenon in which liquid metal shrinks during solidification. Therefore, the solidification shrinkage strain increment $\Delta\varepsilon_{sh}$ shown in Equation (2) is a negative strain that represents shrinkage in the BTR and contributes to solidification cracking. Accordingly, it is necessary to use an index that can evaluate the effect of the solidification shrinkage strain increment on solidification cracking.

In the present study, the plastic strain increment in the BTR $\Delta\varepsilon^{p}_{BTR}$ shown in Fig. 6 is considered as an evaluation index of solidification cracking. As shown in the figure, this represents the difference in plastic strain when the liquidus and solidus temperatures are reached during the cooling process. Note that the weld part can be evaluated as tensile due to the negative strain increment caused by solidification shrinkage strain. In the present study, the plastic strain increment in the BTR was calculated by the thermal elastic-plastic analysis using FEM as follows:

$$\Delta\varepsilon^{p}_{BTR,i} = \sum_{I=n_{t0}}^{n_{t1}} {}^{(I)}\Delta\varepsilon^{p}_{ii} \left(i = x, y, z\right) \tag{3}$$

where t_0 is the solidification start time, t_1 is the solidification completion time, n_{t_0} is the solidification start time step, n_{t_1} is the solidification completion time step, and ${}^{(I)}\Delta\varepsilon^{p}_{ii}$ is the plastic strain increment in direction *i* at time step *I*.

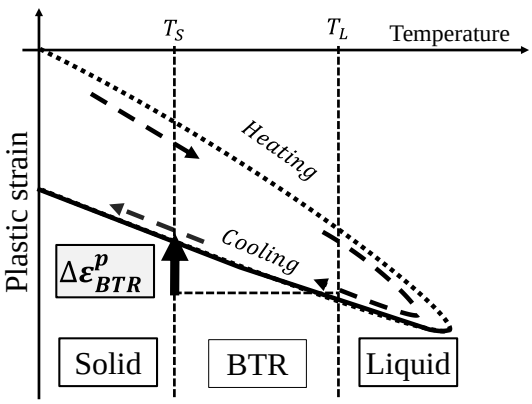

Fig. 6 Schematic illustration of plastic strain increment in BTR during cooling

Solidification cracking is classified into cracking at the position at which the dendrite tips collide and cracking that occurs between neighbouring dendrites. Both types of cracking are considered to be caused by strain perpendicular to the liquid film. In the present study, the plastic strain increment in the BTR during the cooling process was used to evaluate the solidification cracking at the position at which the dendrite tips collide.

SIMPLIFIED PREDICTION OF COLUMNAR CRYSTAL GROWTH DIRECTION

The solidification morphology of molten metal during welding is determined by the temperature gradient and cooling rate and is generally columnar solidification consisting of cells or dendrites [16].

In the research field of metallurgy, the influence of the direction of crystal growth of the molten metal on solidification cracking has been studied. The relationship between the collision angle of columnar crystals and crack initiation has been evaluated based on grain boundary energy [17,18], and it has been reported that solidification cracking is more likely to occur when the collision angle is large [19,20]. In the present study, the direction of solidification growth of columnar crystals and the collision angle between columnar crystals are calculated simply as shown in Fig. 7 using a simplified prediction method for the direction of columnar crystal growth based on the heat conduction analysis using FEM. The direction of growth of columnar crystals in the molten pool is assumed to be the direction of the maximum temperature gradient when each element reaches the BTR in the cooling process, which is defined as the temperature gradient vector in the BTR G_{BTR}:

$$G_{BTR} = \sum_{\alpha=1}^{m} \left(\frac{\partial N^{\alpha}}{\partial x} \boldsymbol{i} + \frac{\partial N^{\alpha}}{\partial y} \boldsymbol{j} + \frac{\partial N^{\alpha}}{\partial z} \boldsymbol{k} \right) T^{\alpha} \tag{4}$$

where N^{α} is the shape function in the FEM, m is the number of nodes per element, i, j and k are basis vectors in the directions, and T^{α} is the temperature of each node when each element reaches the BTR in the cooling process.

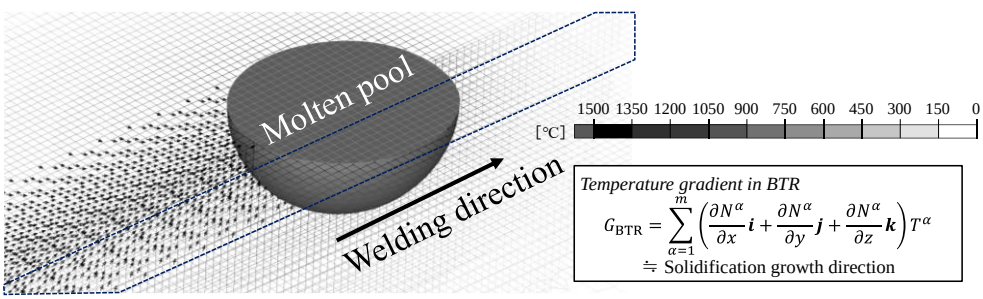

Fig. 7 Temperature gradient vector in BTR for columnar crystal growth direction

By using the temperature gradient vector in the BTR G_{BTR}, the direction of columnar crystal growth can be easily predicted. Furthermore, the position of cracking generation is evaluated using the collision angle of the columnar crystals. It has been reported that the collision angle of columnar crystals has a significant effect on crack initiation [19,20]. Moreover, it is known that solidification cracking is likely to occur where columnar crystals collide and a liquid film which remains over a wide area.

In the present study, the solidification form that is prone to cracking is investigated in the relationship between the temperature gradient vector in the BTR G_{BTR} and the plastic strain increment in the BTR $\Delta\varepsilon_{BTR}^{p}$ generated in the weld zone.

IDEALIZED EXPLICIT FEM

Analysis of solidification cracking requires detailed temperature and strain distribution histories in the weld zone. As such, it is necessary to place fine elements around the melting zone. The IEFEM is an analytical method based on the dynamic explicit FEM that can perform large-scale thermal elastic-plastic analysis at high speed and with little memory [6]. This section provides an overview of the analysis method.

In the IEFEM, the following steps are followed, as shown in Fig. 8.

(1) In the welding transient state, load and temperature increments are applied and the state is maintained.
(2) Calculate the displacement until static equilibrium is reached based on Equation (5) of the dynamic explicit FEM.
(3) When a static equilibrium state is obtained, return to step (1) to calculate the next load step.

$$\left(\frac{1}{\Delta t^2}[M]+\frac{1}{2\Delta t}[C]\right)\{U\}_{t+\Delta t}=\{F\}_t-\sum_{e=1}^{N_e}\int_{V^e}[B]^T\{\sigma\}\,dV + \frac{2}{\Delta t^2}[M]\{U\}_t-\left(\frac{1}{\Delta t^2}[M]-\frac{1}{2\Delta t}[C]\right)\{U\}_{t-\Delta t} \tag{5}$$

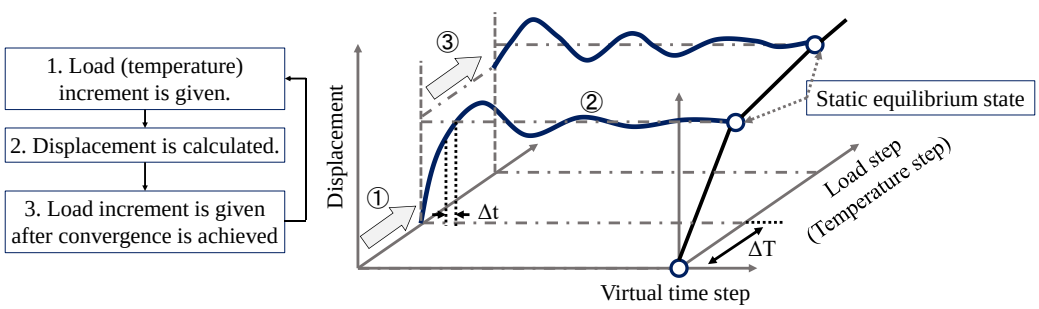

Fig. 8 Schematic illustration of Idealized Explicit FEM (IEFEM)

where [*M*], [*C*], [*B*], and {σ} are the mass matrix, damping matrix, displacement-strain relation matrix and stress vector, respectively. $\{U\}_{t+\Delta t}$, $\{U\}_t$, $\{U\}_{t-\Delta t}$ and $\{F\}_t$ are the displacement vectors at times $t+\Delta t$, t and $t-\Delta t$ and the load vector at time t. Moreover, *Ne* is the number of elements in the analysis model, and *Ve* is the volume of the elements. By making the mass matrix [*M*] and the damping matrix [*C*] nodal-intensive diagonal matrix,

the matrices operations in Equation (5) are no longer simultaneous equations and can be analysed with less memory.

Since the effects of the inertia and damping terms become negligible once the static equilibrium state is obtained by the above calculation procedure, in the process of obtaining the static equilibrium state in the calculation procedure of steps (1) and (2), the mass matrix [*M*] and the damping matrix [*C*] can be adjusted to reduce the time steps required to reach static equilibrium.

By using the above calculation procedure, the IEFEM can be analysed based on the dynamic explicit FEM while considering convergence to a static equilibrium state. The accuracy of the analysis is equivalent to that of the static implicit FEM, while achieving high speed and reduced memory requirements.

APPLICATION OF PROPOSED METHOD TO LARGE-HEAT-INPUT BUTT WELDING

ANALYSIS MODEL AND CONDITIONS

In order to investigate the validity of the solidification cracking analysis method presented in the previous section, the proposed method was applied to large-heat-input butt welding. A JIS G 3106 SM490A steel plate was used as the test specimen. Downward single-sided welding was performed using GMAW. A JIS Z 3313 T49J 0 T5-1 C A-U flux-core wire was used, and a groove filler was sprayed in the groove to stabilize the molten pool. As shown in Fig. 9, the process of joining two steel plates of 600 mm in length, 150 mm in width and 25 mm in thickness by butt welding was studied.

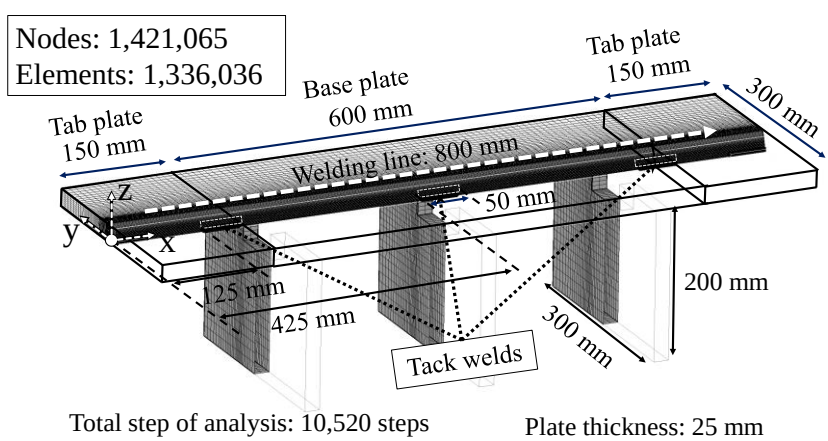

Fig. 9 Shape and size of test plates of butt welding

Tab plates of 150 mm in length, 150 mm in half-width and 25 mm in thickness were attached to the start and end of the base plates. Tack welds of 50 mm in length and 5 mm

in thickness were installed at x = 125 mm, 425 mm and 725 mm, and constraint plates were attached on the opposite side of the welding at x = 200 mm, 440 mm and 680 mm, as shown in Fig. 9 (b). The constraint plate has a U-shape with a width of 300 mm, a height of 200 mm and a thickness of 20 mm. The weld start position is x = 50 mm and the weld end position is x = 850 mm, i.e., the weld length is 800 mm. The 800 mm welding line is divided into 800 elements in the direction of the weld line and unequal elements in the direction of the plate width. The weld part is a V-groove with a 35° groove angle and a root gap of 5 mm. The model shape of the weld metal is based on the experimental cross-sectional macro photograph. The number of nodes and elements are 1,122,416 and 1,059,664, respectively. The current, voltage, welding speed and thermal efficiency were set to 520 A, 43 V, 250 mm/min, and 0.6, respectively, meaning that the heat input is 3,219.8 J/mm. To show the validity of the proposed method, a comparison was made with experimental results under the same conditions. At the start of the heat conduction analysis using FEM, the element corresponding to the weld metal was disabled, and the element was activated when the torch reached the weld during welding. At the beginning of the heat conduction analysis using FEM, the element corresponding to the weld metal was disabled, and the element was activated when the torch reached the weld during welding. The room temperature was set at 20°C.

INVESTIGATION OF PENETRATION SHAPE AND COLLISION ANGLE OF COLUMNAR CRYSTALS

In this section, we investigate the validity of a simple method for predicting the direction of columnar crystal growth. This method is a simplified prediction that assumes the direction of macroscopic epitaxial growth and does not assume the morphology of the base metal, anisotropy in the direction of preferential growth or crystal size. Fig. 10 (a) shows a cross-sectional macro photograph and Fig. 10 (b) shows the penetration shape and the distribution of the temperature gradient vector in the BTR obtained from the heat conduction analysis using FEM. Based on these figures, it can be confirmed that the penetration shape obtained by proposed analysis is in good agreement with the experimental results.

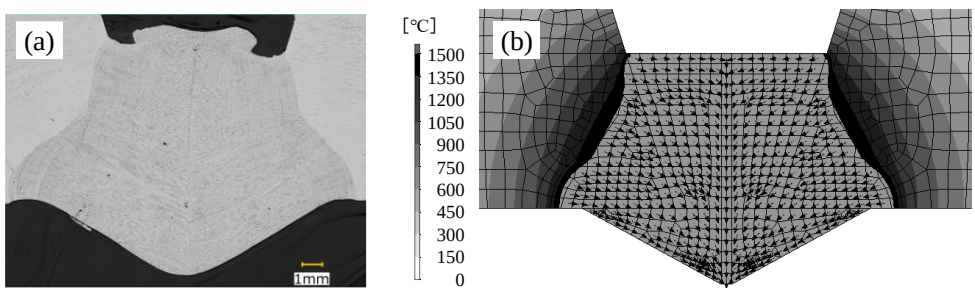

Fig. 10 Penetration shape and direction of columnar crystal growth: (a) Experimental result, (b) Analysis result

The collision angles were calculated at each of the 14 points at which the vertical line passing through the centre of the welding line. The collision angles obtained from experiments and from the temperature gradient vector in the BTR are compared, as shown in Fig. 11.

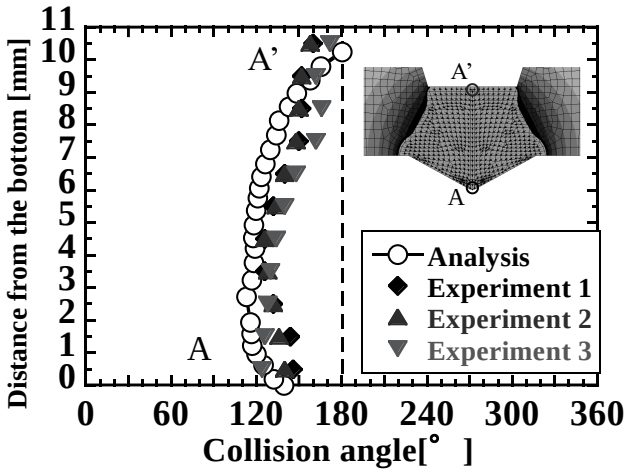

Fig. 11 Collision angle as determined by analysis and experimental results along A-A'

The experimental results were derived from cross-sectional macro photographs obtained from three different cross sections of the same test. The figure shows that the experimental results are highly repeatable with little variation. It can also be seen that the collision angles are close to 180 degrees in the entire plate thickness direction, especially at the upper part, where columnar crystals collide. It can also be found that the distribution trends of the collision angles in the experimental result and analysis results are in good agreement. These results suggest that the temperature gradient vector in the BTR can be used to predict the growth direction and collision angle of columnar crystals with a certain degree of accuracy.

EVALUATION OF SOLIDIFICATION CRACKING INITIATION

In this section, the analysis of the proposed method considering solidification shrinkage strain is performed and compared with the experimental results for the cracking position. Fig. 12 (a) show the distribution of the BTR plastic strain increment in the transverse section at x = 425 mm. Fig. 12 (b) shows the experimental cross-sectional macro photographs at x = 425 mm.

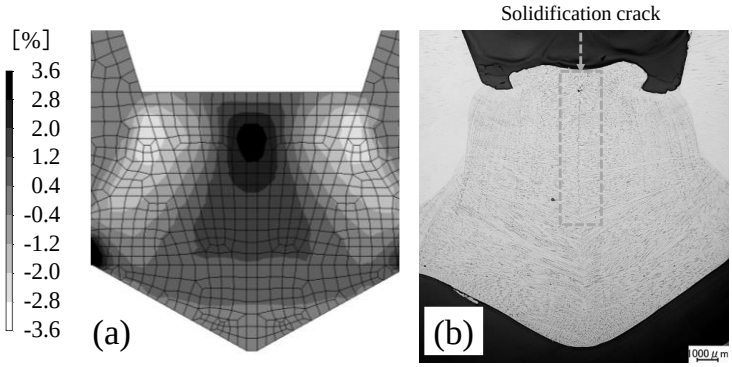

Fig. 12 Distribution of plastic strain increment in BTR and cracking position on transverse cross section at x = 425 mm: (a) Analysis result, (b) Experimental result

In this figure, large tensile plastic strain increment in the BTR of approximately 3.0% is observed at the upper part. As shown in Fig. 12 (b), the experimental results show that cracking occurs at the upper part, and the cracking position is in good agreement with the position of the large tensile plastic strain increment in the BTR obtained by using the proposed method.

Fig. 13 (a) shows the distribution of the plastic strain increment in the BTR in the longitudinal section along the welding line, and Fig. 13 (b) shows the cracking position in the experiment. In Fig. 13 (a), a large plastic strain increment in the BTR can be observed over a wide area behind the tack weld position at the middle and end of the welding line. In addition, from Figs. 13 (a) and 13 (b), it is shown that cracking occurs at the same locations as those with a large plastic strain increment in the BTR. From these figures, it is found that the proposed method can evaluate solidification cracking initiation in the longitudinal direction as well.

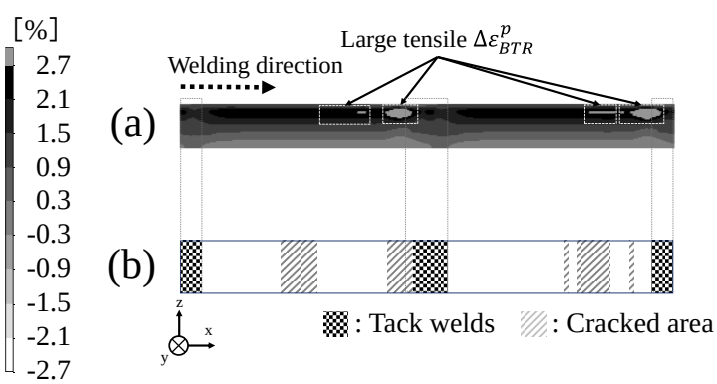

Fig. 13 Distribution of plastic strain increment in BTR and experimentally obtained cracking position: (a) Analysis result, (b) Experimental result

In the above results, it was shown that the proposed method can predict the crack position in both the thickness direction and the longitudinal direction in the solidification cracking evaluation.

EFFECT OF SOLIDIFICATION MORPHOLOGY ON CRACK INITIATION

In this section, the effect of solidification shrinkage strain on the distribution of plastic strain increment in the BTR is examined. As described above, in the transverse section at x = 425 mm, the crystals collided in the upper part, which is a cracking-prone solidification condition.

Analyses were conducted using the conventional method without considering solidification shrinkage strain and the proposed method with solidification shrinkage strain. Fig. 14 shows the distribution of the plastic strain increment in the BTR along line A-A' of the cross section at x = 425 mm for the comparison of the influence without or with solidification shrinkage strain.

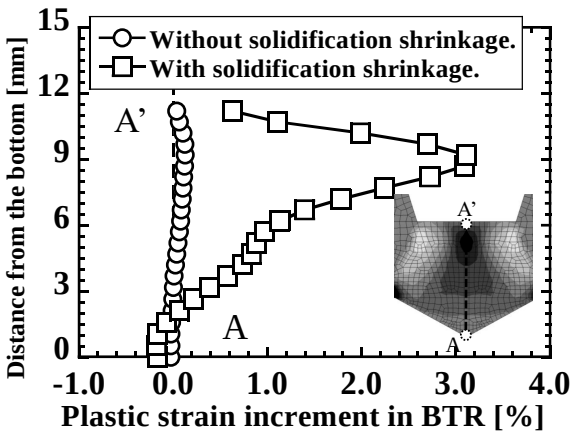

Fig. 14 Influence of solidification shrinkage on plastic strain increment in BTR along A-A'

Fig. 14 shows that the effect of solidification shrinkage strain is not uniform throughout the weld metal, but rather varies depending on the cooling conditions at each position. With the conventional method that does not consider solidification shrinkage strain, it can be confirmed that a tensile plastic strain increment in the BTR of less than 0.2% is distributed throughout the entire plate thickness direction. With the proposed method, which takes into account the solidification shrinkage strain, a large tensile plastic strain increment in the BTR of approximately 3.0% can be confirmed at the upper part. In other words, a large plastic strain increment in the BTR was generated due to the large influence of solidification shrinkage strain at upper part.

Fig. 15 shows the temperature distributions on lines X-X' and Y-Y' in the figure at the start of solidification. Line X-X' is located at the upper part where the crystals collide, and

line Y-Y' is located at the backside where a small plastic strain increment in the BTR is generated.

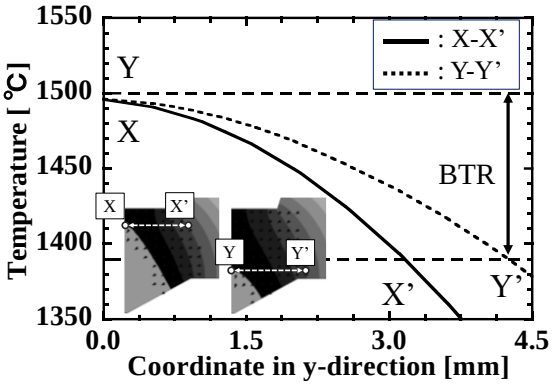

Fig. 15 Temperature distribution in transverse cross section at the start of solidification at x =425 mm

Fig. 15 shows that the temperature gradient in the width direction is large on line X-X' at the upper part, i.e., the distance from the region of the solid phase where stiffness is recovered to the BTR is small. On line Y-Y' of the backside of the weld metal where the collision angle is smaller, the temperature gradient in the width direction is small, i.e., the distance from the region of the solid phase to the BTR is large. In other words, when solidification shrinkage occurs at the upper part of the weld metal, there is greater restraint from the region of solid phase. This is considered to cause cracking susceptibility, due to the greater effect of solidification shrinkage strain.

The above suggests that solidification cracking is likely to occur at the position at which columnar crystals collide, because the effect of solidification shrinkage strain becomes large due to the large surrounding restraints.

CONCLUSIONS

In the present study, a new evaluation method for solidification cracking initiation based on the thermal elastic-plastic analysis using FEM considering mechanical and metallurgical factors is proposed. As metallurgical factors, the direction of solidification growth was simply predicted using the temperature gradient vector in the BTR, and the cracking position was evaluated based on the collision angle of columnar crystals. Analysis was also conducted considering solidification shrinkage strain based on the relationship between temperature and solid fraction in the BTR. From a mechanical point of view, the strain generated in the weld zone was evaluated using the plastic strain increment in the BTR. Furthermore, the proposed method was applied to large-heat-input butt welding.

The results showed the validity of a simple evaluation method for the direction of columnar crystal growth using the temperature gradient vector in the BTR and a

solidification cracking evaluation method using the plastic strain increment in the BTR. This indicates that the proposed method can be used to predict the cracking position.

In addition, it was found that the position at which the collision angle is close to 180° and the crystals collide provides greater restraint against solidification shrinkage, suggesting that the tensile strain at the weld is large, i.e., such solidification morphology is prone to solidification cracking.

References

[1] Y. OKUMOTO: 'Applications of Welding and Joining Technology (Shipbuilding)', *Journal of the Japan Welding Society*, Vol. 79, No. 6, pp. 593-598, 2010.

[2] K. HOSOI and N. HARA: 'Cracking of Welded Joint', *Journal of the Japan Welding Society*, Vol. 78, No. 6, pp. 555-561, 2009.

[3] T. SENDA, F. MATSUDA, G. TAKANO, K. WATANABE, T. KOBAYASHI and T. MATSUZAKA: 'Study on Solidification Crack Susceptibility for Weld Metals with Trans-Varestraint Test (1)', *Jornal of the Japan Welding Society*, Vol. 41, No. 6, pp. 709-723, 1972.

[4] N. N. PROKHOROV: 'The Technical Strength of Metals while Crystallising during Welding', *Welding Production*, Vol. 9, No. 4, pp. 1-8, 1962.

[5] W. S. PELLINI: 'Strain Theory of Hot Tearing', *Foundry*, Vol. 80, pp. 125-199, 1952.

[6] K. IKUSHIMA and M. SHIBAHARA: 'Development of Analytical Method for Welding mechanics Using Idealized Explicit FEM', *Transaction of JWRI*, Vol. 39, No. 2, pp. 384-386, 2010.

[7] *Project of Integrity Assessment of Flawed Components with Structural Discontinuity (IAF) Material Properties Data Book at High Temperature for dissimilar metal welding in Reactor Pressure Vessel*, Japan Nuclear Energy Safety Organization, pp. 120-128, 2013.

[8] T. W. CLYNE, M. WOLF and W. KURZ: 'The Effect of Melt Composition on Solidification Cracking of Steel with Particular Reference to Continuous Casting', *Metallurgical and Materials Transaction B*, Vol. 13, pp. 259-266, 1982.

[9] P. J. WRAY: 'Predicted Volume Change Behaviour Accompanying the Solidification of Binary Alloys', *Metallurgical and Materials Transaction B*, Vol. 7, pp. 639-646, 1976.

[10] N. CONOGLIO and C. E. CROSS: 'Towards Establishment of Weldability Testing Standards for Solidification Cracking', *Cracking Phenomena in Welds IV*, pp. 37-66, 2016.

[11] *Mechanical Engineering Handbook B-2-5 and 7*, Japan Society of Mechanical Engineers, 1984.

[12] M. RAPPAZ, J. M. DREZET and M. GREMAUD: 'A New Hot-Tearing Criterion'. *Metall Mat Trans. A*, Vol. 30, No. 2, pp. 449-455, 1999.

[13] YOKOYAMA T, UESHIMA Y, MIZUKAMI H. KAKIMI and M. KATO: 'Effect of Cr, P and Ti on Density and Solidification Shrinkage of Iron', *Tetsu-to-Hagane*, Vol. 83, No. 9, pp. 557-562, 1997.

[14] H. MIZUKAMI, S. HIRAKI, M. KAWAMOTO and T. WATANABE: 'Tensile Strength of Carbon Steel during and after Solidification', *Tetsu-to-Hagane*, Vol. 84, No. 11, pp. 763-769, 1998.

[15] F. MATSUDA: 'Hot Cracking in Welded Joints of Steels', *Sanyo Technical Report*, Vol. 5, No. 1, pp. 8-19, 1998.

[16] M. GAUMANN and W. KURZ: 'Why is it so difficult to produce an equiaxed microstructure during welding?', *Presented at the Mathematical Modelling of Weld Phenomena Conference*, Vol. 4, pp. 125-136, 1997.

[17] P. RONG, N. WANG, L. WANG, R.N. YANG and W. J. YAO: 'The influence of grain boundary angle on the hot cracking of single crystal superalloy DD6', *Journal of Alloys and Compounds*, Vol. 671, No. 15, pp.181-186, 2016.

[18] N. WANG, S. MOKADEM, M. RAPPAZ and W. KURZ: 'Solidification cracking of superalloy single- and bi-crystals', *Acta Materialia*, Vol. 52, No. 11, pp. 3173-3182, 2004.
[19] J. MELLENTHIN, A. KARMA and M. PLAPP: 'Phase-field crystal study of grain-boundary premelting', *Physical Review B*, Vol. 78, paper no. 184110, 2008.
[20] S. OSHITA, N. YURIOKA, N. MORI and T. KIMURA: 'Prevention of Solidification Cracking in Very Low Carbon Steel Welds', *WJ Research Supplements*, pp. 129s-136s, 1983.